Proceedings of the Combustion Institute, Vol. 33, 2011, pp.2343-2349
S. Maeda, R. Inada, J. Kasahara, and A. Matsuo

1. Title:

Visualization of the Non-Steady State Oblique Detonation Wave Phenomena
Around Hypersonic Spherical Projectile

2. Authors and affiliations:

SHINICHI MAEDA[1], RYUICHI INADA[1], JIRO KASAHARA[1] AND AKIKO MATSUO[2]

[1]*Department of Engineering Mechanics and Energy*
University of Tsukuba
1-1-1 Tennodai, Tsukuba, 305-8573, Japan
[2]*Department of Mechanical Engineering*
Keio University
3-14-1 Hiyoshi,Kohoku-ku, Yokohama, 223-8522, Japan

3. Corresponding author's complete contact information:

Mailing address:
Jiro KASAHARA, Department of Engineering Mechanics and Energy
University of Tsukuba, 3D bldg. room 116, 1-1-1 Tennodai, Tsukuba, 305-8573, Japan
Fax: 029-853-5267
Email: kasahara@kz.tsukuba.ac.jp

4. Colloquium that describes the research topic:

DETONATIONS, EXPLOSIONS AND SUPERSONIC COMBUSITON including pulse-detonation and scramjet engines.

5. Total length of paper and method of determination:

5811 words (method 1)

6. List word equivalent lengths for main text, nomenclature, references, each figure with caption, and each table:

main text: 2941 words
references: 542 words
tables: 76 words
figures: 2252 words

Abstract

We studied experimentally the shock waves and combustion waves generated by a hypersonic spherical projectile in an explosive mixture. An acetylene / oxygen mixture diluted with argon ($2C_2H_2 + 5O_2 + 7Ar$) was used with various initial pressures (detonation cell sizes) to observe optically with a shadowgraph imaging system a shock-induced combustion (SIC), a stable oblique detonation wave (ODW), and a wave called a Straw Hat type consisting of a strong SIC and ODW. The criticality of stabilizing an ODW around a projectile is expressed by the ratio of the projectile diameter, d, to the cell size, λ, as $d / \lambda = 3.63 \sim 4.84$. Although the Straw Hat type wave in the vicinity of criticality is an unstable phenomena, it has been mainly observed by a single frame picture to date, so that it is difficult to discuss the time history of its wave structure. In this study, it was remarkable to directly carry out continuous optical observations using a high speed video camera which can continuously film 100 pictures with a 1 μs frame speed so as to allow an investigation of the sustaining mechanism of the unstable wave structure. Our results allowed the identification of an increase in unsteadiness in the relative distance between the projectile fronts and the transition points to an ODW as the time increased. They also showed local explosions in the SIC region near transition point transformed the ODW front upstream.
(239 words)

Keywords

Hypersonic Projectiles, Oblique Detonation Waves, Detonation Initiation

Introduction

A large variety of colleges, companies, and research organizations are directing attention to applying detonation waves (Kailasanath [1]) to the combustion process of internal combustion engines. In the configuration for generating planar detonation waves in a cylindrical tube, Pulse Detonation Engines (PDEs) (Kailasanath [2]) are prevalent and can generate force and work even if the compressor mechanism is simplified or fully eliminated. They can achieve theoretically a higher thermal efficiency than those that use constant-pressure combustion. For this advantage, their application as an alternative combustor in conventional rockets and air-breathing and gas turbine engines has been investigated experimentally, numerically, and theoretically (Kasahara et al. [3-5], Sato et al. [6], Endo et al. [7, 8]).

On the other hand, applications using stabilized shock-induced combustion (SIC) and self-sustained oblique detonation waves (ODW) (Lehr [9], Li et al. [10]) around projectiles are proposed for oblique detonation wave engines (ODWEs) (Powers [11]) and a Ram-Accelerator (RAMAC) (Hertzberg et al. [12], Higgins [13]). The fundamental researches on these phenomena include both experimental and numerical ones. Matsuo et al. [14, 15] conducted unsteady computational simulations about SIC around hypersonic projectiles called large-disturbance regimes, which have a comparatively long period of combustion cell generation. Additionally, a number of studies about ODW stabilized a wedge have been conducted numerically. Choi et al. [16, 17] revealed that the ODW front becomes unstable and displays cell-like points under conditions of an increase in the activation energy of the mixture. They also investigated a different regime of SIC resulting from length relations between the fluid dynamic time and the chemical time behind a shock wave under a flow-turning angle greater than the maximum attach angle of the ODW. Fusina et al. [18] studied numerically the stability of a wedge supported ODW near the Chapman-Jouguet (C-J) point in an inhomogeneous fuel-air mixture that introduced artificially small disturbances consisting of pure air. A numerical study conducted by Walter et al. [19] was on the interaction between the leading C-J ODW stabilized on a finite length wedge and expansion waves that generated from a wedge shoulder. Together, many experimental studies were conducted to elucidate the criticality of “initiating” or “stabilizing” detonation waves by hypersonic projectiles as being necessary for application to these engines. These studies used a two-stage light-gas gun to launch projectiles at a hypervelocity higher than the C-J velocity on explosive mixtures and took visible images by using Schlieren or Shadowgraph techniques. Kaneshige and Shepherd [20] fired a stoichiometric hydrogen / air mixture diluted with nitrogen with a spherical projectile of 25 mm diameter and projection velocity of 2700 m/s. As an expression of the criticality of initiating and stabilizing the detonation wave, the wave curvature and reaction zone thickness of a mixture was suggested. Higgins [21, 22], and Higgins and Bruckner [23] studied the criticality of the initiation of the detonation in a combustor by projectiles using a pressure history inside a tube. Kasahara et al. [24] launched cylindrical projectiles having conical noses into hydrogen / oxygen and hydrogen / air mixtures, and discussed the criticality of the projectile nose angle and initial mixture pressure. Additionally, an acetylene / oxygen mixture highly diluted with krypton was fired by spherical projectiles with 4.763 mm diameter [25]. It is remarkable to achieve a substantially low C-J velocity (1220 m/s) and a wide range (V_p / D_{CJ} = 1.0～1.8) for the ratio of the projectile velocity, V_p, to the C-J detonation velocity, D_{CJ}. Kasahara et al. integrated experimental data using parameters which are expressed by V_p / D_{CJ} and the ratio (d / λ) of the projectile diameter, d, to the detonation cell size, λ. However Lee [26] proposed an “initiation” criticality using a cylindrical, strong blast-wave analogy, Kasahara et al. suggested a semi-empirical “stabilization” criticality

equation in which the criteria of d / λ proportionally increases to V_p / D_{CJ} in the region $V_p / D_{CJ} > 1$. Above and below the values of the criteria mentioned above, it is observed three types of the waves, a SIC in which shock and combustion wave was decoupled, a wave consisting of SIC in which shock and combustion wave was partially coupled and ODW (they called it the "Straw Hat type"), and stabilized ODW in References 24 and 25. Especially, the Straw Hat type wave was observed in the vicinity of the criteria in which the wave structure makes drastic changes from SIC to ODW. Kasahara et al. discussed the instability of the ODW region by making observations at four points in the projectile flight direction, each with a different experiment in Ref. 24. Although the Straw Hat type is presumably an unstable phenomenon, it has been mainly observed by a single frame picture to date; there is no result to our knowledge from direct observations providing a detailed time history.

At the present time, the development of Electro-technology has allowed the filming of 100 pictures continuously with a 1 μs frame speed. We have elucidated a sustained mechanism for the unstable Straw Hat type phenomena and identified the criticality for stabilizing the ODW by directly carrying out optical observations of continuous frames.

Experimental Setup and Condition

Our experimental setup consists of four devices, shown in Fig. 1. First, there is a two-stage light-gas gun which can launch a spherical projectile at about 2300 m/s. Second, an observation chamber with glass windows which is filled with an explosive mixture, shown between diaphragm 1 and 2 in Fig. 1. Third, a Shadowgraph imaging system for observation of the wave structure around the projectile. Fourth, an evacuation chamber for capturing the projectile and burned gas. To film the projectile, we used a high speed video camera HPV-1 (312 × 260 pixels resolution, SHIMADZU) which can film 100 pictures continuously with a 1 μs frame speed and 250 ns exposure time. Through the glass window at 200 mm upstream from the observation section center, a He-Ne laser was set to pass the flight trajectory of a projectile. On the opposite side of the laser, the output is measured with a photodiode, which detects the signal for intercepting the passing projectile and triggers the start of camera recording.

In this study, we used a stoichiometric acetylene / oxygen mixture diluted with argon in a 50% volumetric fraction ($2C_2H_2 + 5O_2 + 7Ar$), and we changed the initial filling pressure p_0 = 21.1 kPa to 60.7 kPa and kept an almost constant temperature T_0 = 283.9 ± 2.5 K. The projectile is a sphere with a 4.763 mm diameter; its velocity was 2260 ± 130 m/s, which is always higher than the C-J detonation velocity of the mixture.

To express the critical condition needed to generate a stable oblique detonation wave around the projectile, it is necessary to give the detonation cell size λ which is the width of the each cell structure perpendicular to the direction of the wave propagation. Kaneshige and Shepherd [27] compiled a detonation database that includes cell size data for various mixtures. Here, we used Desbordes's [28] results for the same mixture in p_0 = 3.96 kPa to 35.6 kPa and T_0 = 293 K, and the fitting equation (1) for these results as an exponential of p_0. In the equation, p_0 and λ are kilopascals and millimeters, respectively. We used equation (1) to extrapolate λ corresponding to our experimental conditions.

$$\lambda = 61.52 \times p_0^{-1.117} \qquad (1)$$

for $2C_2H_2 + 5O_2 + 7Ar$

It could determine the normal velocity component of the detonation wave D_{CJ} for the conditions in which we could observe a stable C-J oblique detonation wave around the projectile. Our experiments had an observation

region 90 mm in diameter, and we could film the projectile in 40 μs frames (40 pictures) and could observe that the wave remains steady in this region. D_{CJ} is calculated by

$$D_{CJ} = V_p \sin \theta_{CJ} \qquad (2)$$

where, V_p is the projectile velocity and θ_{CJ} is the wave angle of a C-J oblique detonation wave. The measured D_{CJ} was about 1950 m/s and agreed within 7% differences with the value calculated by STANJAN chemical thermodynamics software (Reynolds [29]). The projectile velocity V_p was calculated by scanning its location time history from continuous pictures filmed by a high speed camera. The projectile location changed almost linearly against time in all experimental conditions. Therefore, V_p was taken as the gradient of straight line passing the first and last points of the projectile location in the observation region. The significantly short frame speed of 1 μs gives better projectile location information than the method using laser cutting. The systematic error of D_{CJ} was 0.65 %. The experimental conditions are listed in Table 1.

Criticality for Stable C-J Oblique Detonation Wave at Various Initial Pressures for the Mixture

In this study, projectile velocities were almost constant at about 2300 m/s, and the initial pressures (detonation cell sizes) of the mixture were changed. The pictures in the filmed movie for each condition are shown in Fig. 2; they are negative pictures for clarity. For comparison, Fig. 2 (a) is a result of launching a projectile into argon, an inert gas. Herein, we discuss the criticality of using the ratio of the projectile velocity, V_p, to the C-J detonation velocity, D_{CJ}, V_p / D_{CJ}, and the ratio of the projectile diameter, d, to the detonation cell size, λ, d / λ, as suggested in Ref. 25. We varied d / λ from 2.34 to 7.61 while maintaining $V_p / D_{CJ} = 1.14 \pm 0.07$. We observed in Fig. 2 (b) at $d / \lambda = 2.34$, that there was a SIC in which a bow-shock and combustion wave were decoupled; in Figs. 2 (d) and (e) at $d / \lambda = 4.84$ and 7.61, that there was a stable ODW; and in Fig. 2 (c) at $d / \lambda = 3.63$, that there were SIC in which the bow-shock and combustion wave were partially coupled and the ODW at a certain downstream region (which was called the Straw Hat type in Ref. 25). From these observations, we consider the criticality to stabilize ODW to be $d / \lambda = 3.63$ to 4.84; it approximates the result of Kasahara et al. (which was $d / \lambda = 5.01$).

Regarding the wave front shape of the Straw Hat type, it seems that the angle of the shock wave and projectile traveling axis widely changes at the transition point from SIC to ODW. In Ref. 25, two projectile velocity conditions at $V_p / D_{CJ} = 1.10$ and 1.62 showed the Straw Hat type in a single frame picture; the latter condition apparently had small angle changes. Herewith, it might consider that the condition for the occurrence of the Straw Hat type is determined by the criteria d / λ, and the wave front shape changes corresponding to V_p / D_{CJ}.

Figs. 2 (c), (d) and (e) show the ODW, but the downstream regions of the wave front are different. In Figs. 2 (c) and (d), the striped patterns are visible as a result of the cell structure of the detonation wave, although they cannot be seen clearly in Fig. 2 (e). This difference might be explained by examining the difference in the detonation cell sizes. By using equation (1), the conditions in Figs. 2 (c) and (d) are $\lambda = 1.31$ and 0.985 mm; on the other hand, Fig. 2 (e) is $\lambda = 0.627$ mm. Because the imaging resolution was 0.3 mm/pixel and more than 3 pixels is necessary to display striped patterns, the patterns cannot be seen in Fig. 2 (e).

Finally, we notice a wave generated by a wake behind the projectile. In each picture of Fig. 2, the wave locations (shown in white arrows) at the same distance from the projectile front edge are shown. Some of them are not clearly visible, however, we could see them in all continuous pictures, not only in a picture showed in Fig. 2. Compared with Fig. 2 (a) for the argon, Figs. 2 (b) to (e), which involve chemical reactions, have large angles for

the wave and projectile traveling axis. Especially, the cases observed of the ODW in Figs. 2 (c), (d) and (e) are remarkable; the angle increases at higher initial pressures. It is considered that the burned gas expands downstream from the detonation waves and extends the regions which are affected by the wake.

Time History of Wave Structure below Criticality

Fig. 3 shows continuous pictures of the SIC observed at the condition $d / \lambda = 2.34$. It shows $t = 24 \sim 44$ μs at 4 μs intervals and $t = 0$, the start of camera recording. In the neighborhood of the projectile, there are visible pressure disturbances caused by combustion cells in the combustion regions of the decoupled shock wave. Again, it seems that, regardless of the times, waves caused a projectile wake arise from the combustion regions downstream from the projectile, and the locations (shown in white arrows) remain at the constant value 30 ± 2 mm from a projectile front. Downstream from these points, the combustion regions are fully enfolded by wakes, and pressure disturbances caused by combustion cells are not clear in these regions.

Fig. 4 shows continuous pictures of the Straw Hat type observed at the condition $d / \lambda = 3.63$. The left line shows $t = 22 \sim 26$ μs at 1 μs intervals with $t = 0$, the start of camera recording, and the right line shows $t = 30 \sim 46$ μs at 4 μs intervals. Although the SIC regions in the vicinity of a projectile and the ODW regions at certain places downstream propagate steadily, the intersections of both regions are unsteady, with repeating strong explosions on the upper and lower sides of the projectile. The SIC and ODW regions can be interpreted with or without the striped patterns that are caused by the cell structure. The distances Δx_{tr} between the projectile front and these transition points are plotted in Fig. 5 in different parts for the upper and lower sides of a projectile, and errors are shown according to the spatial resolution. As is also visible in Fig. 4, the transition point for the lower side exists downstream than for the upper side. However, the Δx_{tr} increases for both sides as the time increases; on the upper side, it is observed that the transition point moves upstream during $t = 23$ μs to 24 μs. The left line of Fig. 4 shows detailed time history of these phenomena. After a strong explosion occurs on the upper side, a new oblique detonation wave front is visible longitudinally at $t = 24$ μs. At this time, other shock waves, in addition to the waves that caused the wake, have developed downstream from this transition point. In this study, we directly observed the phenomena which were suggested in Ref. 24; that a ODW of the Straw Hat type slides back relative to the projectile location as the time increases. Additionally, it is confirmed that the unsteady phenomena of strong local explosions in the SIC region moving the ODW front upstream, rather than sliding back continuously. We highlighted in observation of Straw Hat type about this wave structure didn't be disrupted instantaneously as a transition phenomenon, but had almost constant wave structure during passing the observation region (it had 90mm diameter, and observation duration was about 40μs). Therefore, we suggested that Straw Hat type was generated soon after a projectile running into a combustion chamber and propagated with maintaining its wave structure. In Reference [20], it was observed that an explosion appeared at projectile upper side and lower side simultaneously certain downstream SIC region around projectile. And this process was described as instantaneous DDT process. Meanwhile, Straw Hat type observed in this study might have apparently different propagation mechanism.

Conclusions

With changes in the initial filling pressure, a spherical projectile was fired with a velocity of 2300 m/s using a two-stage light-gas gun into an acetylene / oxygen mixture diluted with argon. With a Shadowgraph imaging

system and high-speed video camera, we observed optically at a 1 μs frame speed a shock-induced combustion (SIC), a stable oblique detonation wave (ODW), and a wave called a Straw Hat type that consists of a strong SIC and ODW. The criticality for stabilizing the ODW around a projectile was $d / \lambda = 3.63 \sim 4.84$; it approximates the result of Kasahara et al. ($d / \lambda = 5.01$). Considering the phenomena of the shock-induced combustion and the Straw Hat type wave at a condition below criticality, the following phenomena were directly confirmed. In the shock-induced combustion, it seems that, regardless of the times, the waves caused a projectile wake arise from the combustion regions downstream from the projectile, and the locations remain at the constant value 30 ± 2 mm from a projectile front. At the downstream location from this point, the combustion regions are fully enfolded by wakes, and the pressure disturbances caused by combustion cells in this region are not clear. Also, we directly observed phenomena which were suggested by Kasahara et al.; that the ODW of the Straw Hat type slides back relative to the projectile location as time increases. Additionally, it is confirmed that the unsteady phenomena of strong local explosions in the SIC region moving the ODW front upstream, rather than sliding back continuously.

Acknowledgements

This work was subsidized by the Ministry of Education, Culture, Sports, Science and Technology, a Grant-in-Aid for Scientific Research (A), No. 20241040; a Grant-in-Aid for Scientific Research (B), No. 21360411; and Research Grant Program from the Institute of Space and Astronautical Science, the Japan Aerospace Exploration Agency.

References

[1] K. Kailasanath, AIAA J. 38 (9) (2000) 1698-1708.

[2] K. Kailasanath, AIAA J. 41 (2) (2003) 145-159.

[3] J. Kasahara, M. Hirano, A. Matsuo, Y. Daimon, T. Endo, J. Propul. Power 25 (6) (2009) 1281-1290.

[4] J. Kasahara, A. Hasegawa, T. Nemoto, H. Yamaguchi, T. Yajima, T. Kojima, J. Propul. Power 25 (1) (2009) 173-180.

[5] J. Kasahara, Z.Liang, S. T. Browne, J.E. Shepherd, AIAA J. 46 (7) (2008) 1593-1603.

[6] S. Sato, A. Matsuo, T. Endo, J. Kasahara, J. Propul. Power 22 (1) (2006) 64-69.

[7] T. Endo, J. Kasahara, A. Matsuo, K. Inaba, S. Sato, T. Fujiwara, AIAA J. 42 (9) (2004) 1921-1929.

[8] T. Endo, T. Yatsufusa, S. Taki, A. Matsuo, K. Inaba, J. Kasahara, J. Propul. Power 23 (5) (2007) 1033-1041.

[9] H.F. Lehr, Astronautica Acta 17 (1972) 589-597.

[10] C. Li, K. Kailasanath, E.S. Oran, Phys. Fluids 6 (4) (1994) 1600-1611.

[11] J.M. Powers, Combustion in High-Speed Flows, Kluwer Academic Publishers, Boston, 1994, p.345-371.

[12] A. Hertzberg, A.P. Bruckner, D.W. Bogdanoff, AIAA J. 26 (2) (1998) 195-203.

[13] A.J. Higgins, J. Propul. Power 22 (6) (2006) 1170-1187.

[14] A. Matsuo, K. Fujii, AIAA J. 33 (10) (1995) 1828-1835.

[15] A. Matsuo, K. Fujii, AIAA J. 34 (10) (1996) 2082-2089.

[16] J.-Y. Choi, D.-W. Kim, I.-S.Jeung, F. Ma, V. Yang, Proc. Combusti. Inst.31 (2007) 2473-2480.

[17] J.-Y. Choi, E. J.-R. Shin, I.-S.Jeung, Proc. Combusti. Inst.32 (2009) 2387-2396.

[18] G. Fusina, J.P. Sislian, B. Parent, AIAA J. 43 (7) (2005) 1591-1604.

[19] M.A.T. Walter, L.F. Figueira da Silva, AIAA J. 44 (2) (2006) 353-361.

[20] M.J. Kaneshige, J.E. Shepherd, Proc. Combusti. Inst.26 (1996) 3015-3022.

[21] A.J. Higgins, AIAA paper 97-3179.

[22] A.J. Higgins, Investigation of Detonation Initiation by Supersonic Blunt Bodies, PhD thesis, University of Washington, Seattle, 1996.

[23] A.J. Higgins, A.P. Bruckner, AIAA paper 96-0342.

[24] J. Kasahara, T. Fujiwara, T. Endo, T. Arai, AIAA J. 39 (8) (2001) 1553-1561.

[25] J. Kasahara, T. Arai, S. Chiba, K. Takazawa, Y. Tanahashi, A. Matsuo, Proc. Combusti. Inst. 29 (2002) 2817-2824.

[26] J.H.S. Lee, Prog. Astronaut. Aeronaut. 173 (1997) 293-310.

[27] M.J. Kaneshige, J.E. Shepherd, Detonation Database, Technical Report No. FM97-8, GALCIT, Pasadena, CA, 1997.

[28] D. Desbordes, Prog. Astronaut. Aeronaut. 114 (1988) 170-185.

[29] W.C. Reynolds, The Element Potential Method for Chemical Equilibrium Analysis: Implementation in the Interactive Program STANJAN: Version3, Technical Report No. A-3991, Stanford Univ., 1986.

List of figure captions

Table 1: Experimental conditions

Fig. 1: Schematic diagram of the experimental arrangement (top view)

Fig. 2: The snap-shots of observed moving image with various mixture initial pressure (negative photograph) ($V_p/D_{CJ} = 1.14 \pm 0.07$)

(a) Ar, $p_0 = 60.8$kPa

(b) $2C_2H_2 + 5O_2 + 7Ar$, $p_0 = 21.1$kPa, $d / \lambda = 2.34$

(c) $2C_2H_2 + 5O_2 + 7Ar$, $p_0 = 31.4$kPa, $d / \lambda = 3.63$

(d) $2C_2H_2 + 5O_2 + 7Ar$, $p_0 = 40.5$kPa, $d / \lambda = 4.84$

(e) $2C_2H_2 + 5O_2 + 7Ar$, $p_0 = 60.7$kPa, $d / \lambda = 7.61$

Fig. 3: Case in which the Shock-Induced Combustion is observed [Corresponding to Fig.2 (b)]

Fig. 4: Case in which the Straw Hat type is observed [Corresponding to Fig.2 (c)].
Location of oblique detonation wave transitions upstream at $t = 24$ μs and generation of new wave front.
Strong explosion is observed on the upper and lower sides of projectile at $t = 23$, 26 and 38 μs.

Fig. 5: Time history of the distance between projectile front and oblique detonation wave transition point

Table 1
Experimental conditions
(single column: 76 words)

Shot No.	Gas	p_0	T_0	V_p	V_p/D_{CJ}	d/λ
-	-	kPa	K	m/s	-	-
1	Ar	60.8	282.3	2318	-	-
2	2C2H2 + 5O2 +7Ar	21.1	286.4	2340	1.20	2.34
3	2C2H2 + 5O2 +7Ar	31.4	281.4	2333	1.19	3.63
4	2C2H2 + 5O2 +7Ar	40.5	283.4	2386	1.21	4.84
5	2C2H2 + 5O2 +7Ar	60.7	282.3	2133	1.07	7.61

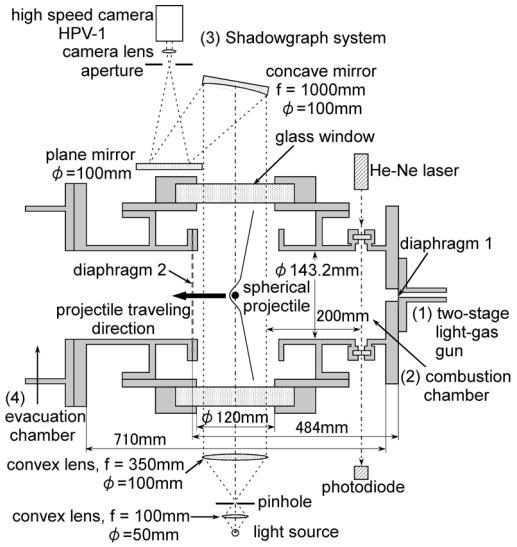

Fig. 1 Schematic diagram of the experimental arrangement (top view)
(single column: 191 words)

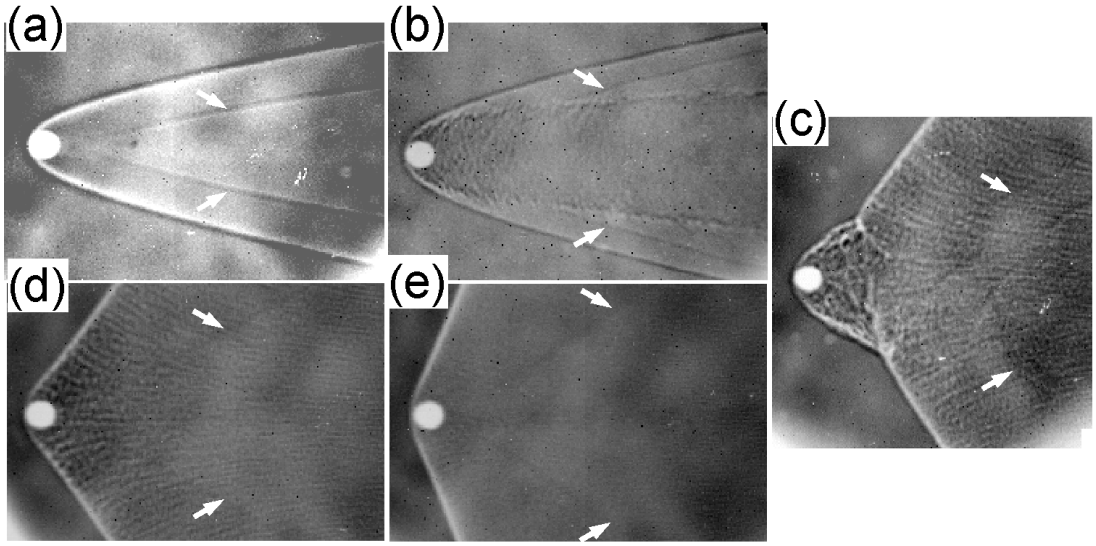

Fig. 2 The snap-shots of observed moving image with various mixture initial pressure (negative photograph)
($V_p/D_{CJ} = 1.14 \pm 0.07$)
(a) Ar, $p_0 = 60.8$kPa
(b) $2C_2H_2 + 5O_2 + 7Ar$, $p_0 = 21.1$kPa, $d / \lambda = 2.34$
(c) $2C_2H_2 + 5O_2 + 7Ar$, $p_0 = 31.4$kPa, $d / \lambda = 3.63$
(d) $2C_2H_2 + 5O_2 + 7Ar$, $p_0 = 40.5$kPa, $d / \lambda = 4.84$
(e) $2C_2H_2 + 5O_2 + 7Ar$, $p_0 = 60.7$kPa, $d / \lambda = 7.61$
(double column: 438 words)

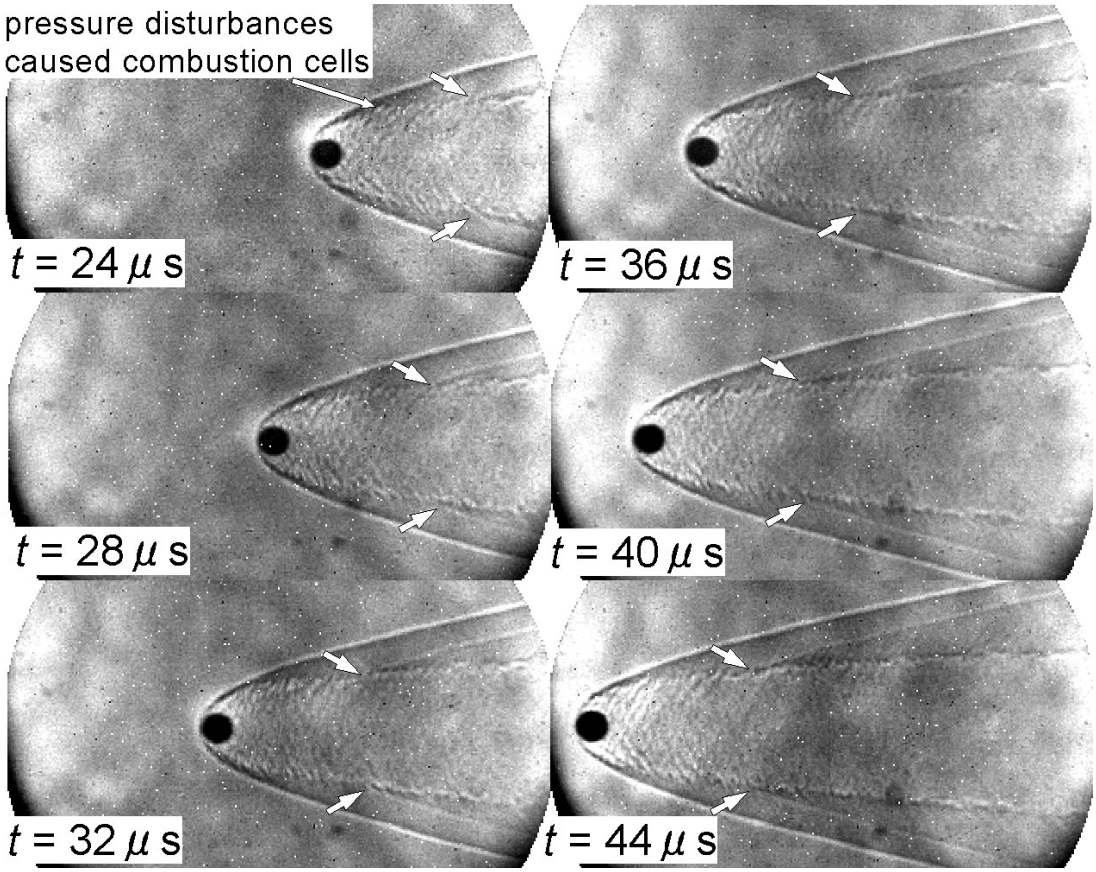

Fig. 3 Case in which the Shock-Induced Combustion is observed [Corresponding to Fig.2 (b)]
(double column: 546 words)

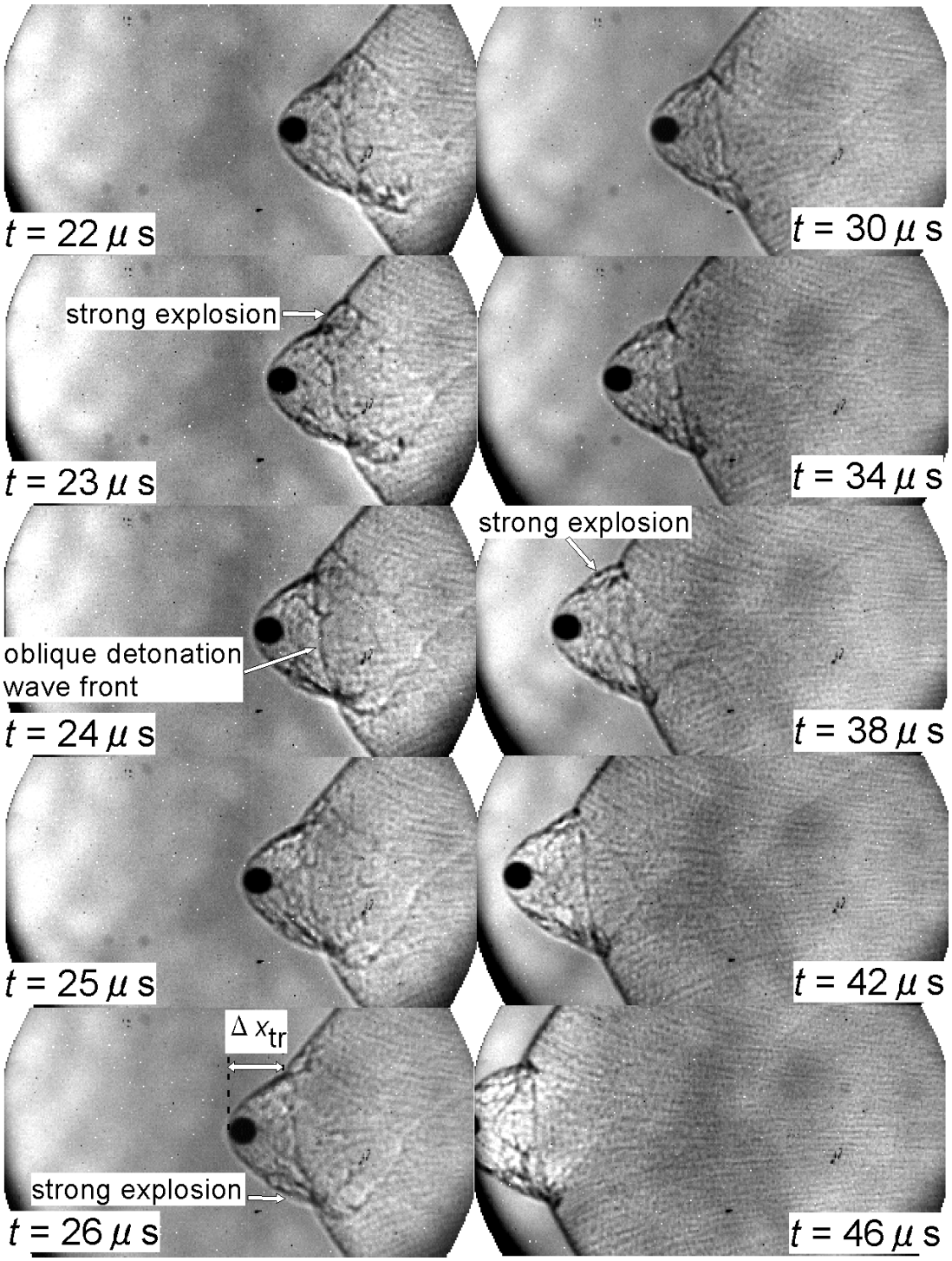

Fig. 4 Case in which the Straw Hat type is observed [Corresponding to Fig.2 (c)].
Location of oblique detonation wave transitions upstream at t = 23 μs and generation of new wave front. Strong explosion is observed on the upper and lower sides of projectile at t = 23, 26 and 38 μs.
(a full page figure: 900 words)

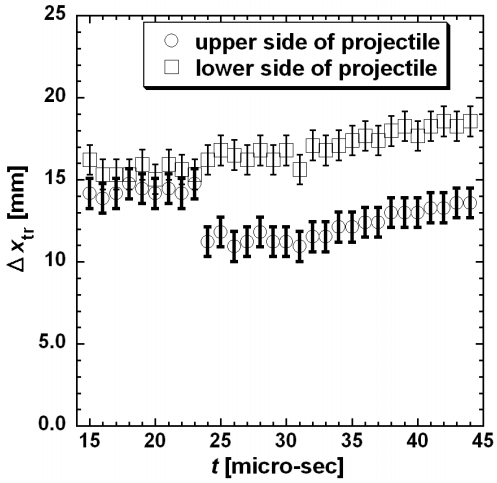

Fig. 5 Time history of the distance between projectile front and oblique detonation wave transition point
(single column: 177 words)